Indian Journal of Chemical Technology
Vol. 26, September 2019, pp. 437-443

Effect of intermetallics of 2219-T87 aluminium alloy on exposure to aggressive media

Venkatasubramanian G*[,1], Sheik Mideen A[2] & Abhay K Jha[3]

[1]Department of Chemistry, JeppiaarMamallan Engineering College, Vadamangalam 602108, Tamilnadu, India
[2]Department of Chemistry, Sathyabama Institute of Science and Technology, Jeppiaar Nagar, Chennai 600119, Tamilnadu, India
[3]Materials Processing Division, Vikram Sarabhai Space Centre, Indian Space Research Organisation, Thiruvananthapuram 695022, Kerala, India
E-mail: *gvsmani2008@gmail.com*

Received 4 November 2017; accepted 2 September 2018

The effect of precipitating agent Al_2Cu intermetallic particles of high strength 2219-T87 aluminum alloy plate (AA2219-T87) used in cryogenic propellant tank for space applications has been investigated on exposure to aggressive media like unsterile natural seawater and 0.6 M NaCl solution. The corrosion resistance of AA2219-T87 plate has been evaluated by long term weight loss method, Tafel polarization and electrochemical impedance spectroscopy (EIS) techniques while the surface morphology of bare and exposed samples have been characterized using scanning electron microscopy (SEM) coupled with energy dispersive X-ray analysis (EDX). The Tafel plots and EIS studies reveal the lower corrosion current and higher charge transfer resistance of AA2219-T87 plate in unsterile natural seawater than in 0.6 M NaCl solution. The SEM with EDX studies confirm that the improved corrosion resistance of AA2219-T87 plate for long term exposure in unsterile natural seawater is mainly attributed to the blocking of cathodic nature of Al_2Cu intermetallic particles by the formation of compact passive film of oxides, carbonates and silicates of calcium and magnesium. The surface studies further confirm that a complete damage of Al_2Cu intermetallic particles in AA2219-T87 plate led to pitting type corrosion on exposure to 0.6 M NaCl solution.

Keywords: AA2219-T87, Weight loss measurement, Potentiodynamic polarisation, EIS, Microstructure

2219 Al-Cu (Al-6.3% Cu) is a high strength precipitation hardenable alloy widely used in the aerospace structures. Aluminium alloy 2219-T87 is readily weldable and successfully used as welded space booster oxidizer tanks, fuel tanks and supersonic aircraft structural components and also useful in applications over a temperature range of –269 to 300°C[1,2]. Particularly in the space transportation system the solid rocket boosters (SRB) are reusable solid motors and the aft skirt is constructed from AA2219-T87 which is a part of SRB. In AA2219, Al_2Cu is the major intermetallic compound, which improves mechanical properties of this alloy but it triggers corrosion due to its cathodic nature with respect to Al matrix to the formation of galvanic cells between the noble Al_2Cu and the Al matrix[1]. Several studies have demonstrated the effect of intermetallics of AA1100[3], AA2024[4], Al-Cu-Zn[5] in passivity breakdown and pit morphology when exposed to seawater. Even in alkaline media, Al–Cu alloys showed very poor pitting corrosion resistance[6]. The effect of S phase particles and Al–Cu–Fe–Mnphase after exposure to NaCl for several hours has been investigated[6,7]. A heavy corrosion around the S phase particles, but minimal activity around the Al–Cu–Fe–Mn phase were observed. The corrosion resistance of AA2219 before and after the removal of copper rich phase was analysed by electrochemical measurements at different time intervals from 24 h to 168 h[8]. The effect of pH on the rate of corrosion of aluminium alloys have also been studied[9-11]. However, the effect of intermetallics of 2219-T87 aluminium alloy for long term exposure in aggressive media has not been systematically investigated. The present investigation envisages the effect of intermetallics of AA2219-T87 aluminium alloy on exposure from 1 day to one year in unsterile natural seawater and 0.6 M NaCl solution.

Experimental Section

Materials

The AA2219 (5.95Cu-0.27Mn-0.12Zr-0.09V-0.06Ti-0.12Fe-0.05Si wt. %) rolled plate in T-87 temper condition[2] was used in the present study. A 3.5

wt. % (0.6 M) NaCl (LobaChemie make, *p*H 6.5, conductance 38.4 mMho) solution and seawater (pH 8.2, conductance 33.9 mMho) collected from East Coast area, Chennai were used as electrolytes. The working electrodes for corrosion studies were cut from the AA2219-T87 in transverse direction parallel to the rolling direction having the area of 8 mm^2. For full immersion tests AA2219-T87 specimen of 1 $inch^2$ were used. Immersion tests were performed in triplicate and the average was taken. All the specimens were used in flat type with mirror smooth finish after mechanically abraded with different grades of silicon carbide sheets followed by 1 μm finish using rotating disc with non-aqueous diamond paste, degreased by acetone, washed with double distilled water and dried. The corrosion rate was calculated using the formula:

$$\text{Corrosion rate in mpy} = \frac{534 \times W}{D \times A \times T}$$

where W is the weight loss in milligrams, D is the density, A is the area in inches and T is the time in hours

Electrochemical Techniques

Potentiodynamic polarisation tests were carried out according to ASTM standard G3-89 using software based Bio-analytical system [BAS-Zahner, IM6 Electrochemical Workstation using Thales software]. The flat type working electrode of AA2219-T87, a saturated calomel electrode (SCE) coupled to a fine Luggin capillary as reference electrode and graphite electrode as counter electrode were used. The Luggin capillary was kept close to the working electrode to reduce the ohmic contribution. The polarisation curves were determined by stepping the potential at a scan rate of 0.5 mV s^{-1} from –250 mV to +250 mV versus open circuit potential (OCP vs SCE). All the experiments were conducted at room temperature (25°C).

The electrochemical impedance spectroscopy (EIS) measurements were carried out using a potentiostat coupled to a frequency response analyzer system in the frequency range of 100 kHz to 100 mHzwith an AC amplitude of 10 mV peak to peak using AC signals at open circuit potential. The same three electrode system was used for this study also. All the experiments were performed at room temperature (25°C) with 10 min time delay to reach steady state in freely aerated condition. All experiments analyzed in this paper were repeated for at least two times for reproducibility.

Surface analysis

The samples immersed in both the media from 1 day to 1 year were periodically removed as per required duration and cleaned with double distilled water and finally with concentrated 15.8 M HNO_3 for about 2-3 min[12]. The weight loss and corrosion rate were calculated after taking final weight. Photographs were taken to reveal the macro structure using NIKON-D80 camera (Japan make) with a resolution of 10 Mega pixels. After removing the samples, the *p*H and conductance of the electrolytes were also noted using the calibrated *p*H meter and conductivity meter. The microstructural characterisation of the samples was carried out by an optical microscope (Olympus GX 71 Inverted Metallurgical Microscope, Japan) and a scanning electron microscope (HITACHI model) coupled with energy dispersive X-ray analysis (EDX).

Results and Discussion

Macrographs and microstructural characterization of AA2219-T87 plate

The photograph of polished AA2219-T87 plate is shown in Fig. 1a which revealed the smooth and bright surface of the alloy. Figs. 1b and 2a showed the metal surface exposed for 24 hours in 0.6 M NaCl solution and seawater respectively. It is observed from the macrographs that the sample immersed in 0.6 M NaCl solution showed huge number of small patches distributed in many places indicating that the alloy is highly susceptible to pitting type corrosion while the sample exposed in seawater showed slight brown in colour indicating the formation of possible passive film formed by divalent metal cations. The same trend has been observed for the samples exposed for one month (Figs. 1c and 2b). Figures 1d and 2c showed the specimen exposed for one year in 0.6 M NaCl and seawater. Before cleaning, the surface of the samples was covered with the various corrosion products. After cleaning with concentrated nitric acid, the samples (Figs. 1e and **2**d) showed huge number of pits and the extent of depth is relatively more in the sample exposed to 0.6 M NaCl solution.

The microstructure of polished surface of AA2219-87 plate (Fig. 3a) showed typical elongated grains in α phase with coarse constituents of $CuAl_2$ intermetallic particles (IMPs)[13,14]. The microstructure of specimens exposed to 0.6 M NaCl solution for 24 h

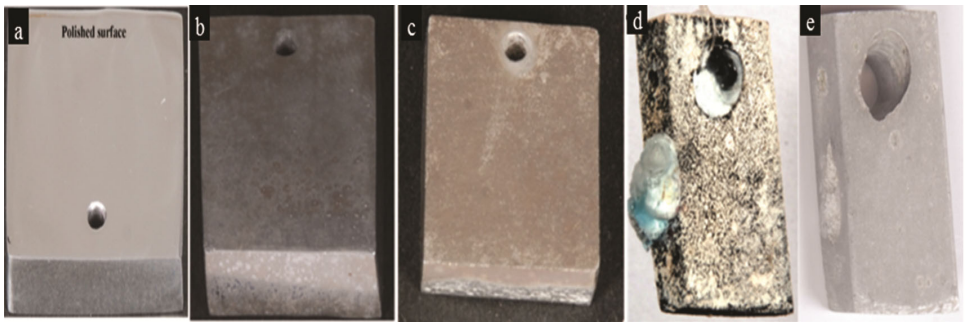

Fig. 1 — (a)Macrograph of polished surface of AA2219-T87 plate; (b) AA2219 plate exposed in 0.6 M NaCl for one day duration; (c) One month duration; (d) One year duration before cleaning and (e) One year duration after cleaning

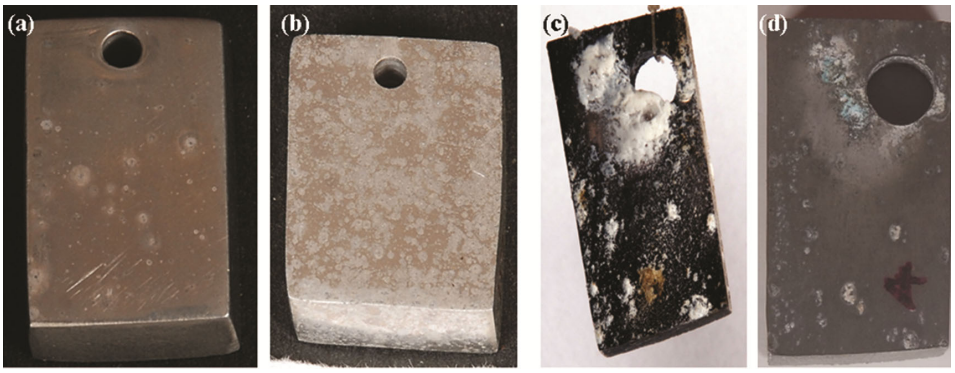

Fig. 2 — Macrograph of AA2219 plate exposed in seawater for (a) One day duration; (b) One month duration; (c) One year duration before cleaning and (d) One year duration after cleaning

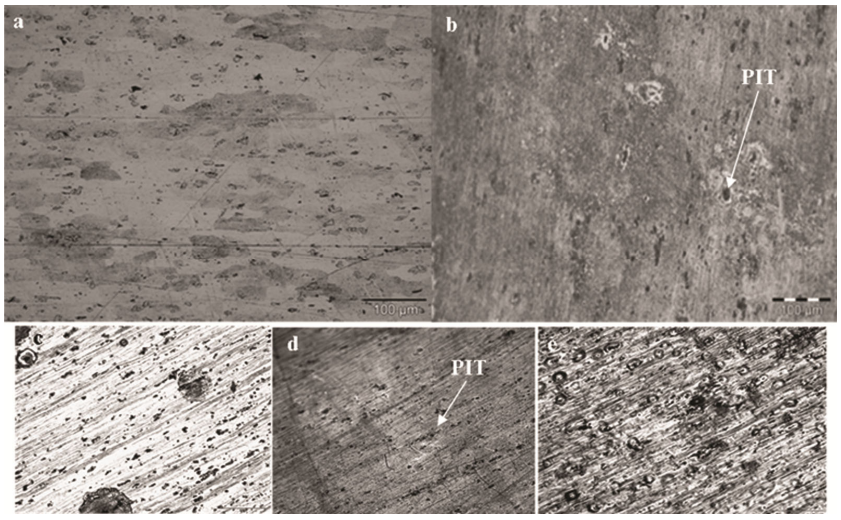

Fig. 3 — (a) Microstructure of polished surface of AA2219-T87 plate; (b) Microstructure of AA2219-T87 plate exposed in 0.6 M NaCl for one day duration; (c) For one month duration; (d) Microstructure of AA2219-T87 plate exposed in seawater for one day duration and (e) For one month duration

and one month duration is shown in Figs. 3b and 3c, respectively. The samples exposed in seawater for 24 h and one month duration is shown in Figs. 3d and 3e respectively. The sample exposed to 0.6 M NaCl solution for 24 h duration showed pits with complete damage of the surface while the sample exposed to seawater is characterised with scattered pits. The formation of pits is caused by the preferential dissolution of IMPs[15]. The same trend has been observed for the samples exposed for one month duration.

The SEM images of AA2219-T87 plate exposed in 0.6 M NaCl and in seawater for one year before cleaning with HNO_3 are depicted in Figs. 4a and 4b,

respectively. The EDX analysis of sample exposed in 0.6 M NaCl solution exhibited pearl like structure indicating the formation of sodium or copper oxides. But the sample exposed in seawater exhibited uniform calcium and magnesium oxides, carbonates over the matrix phase.

Figures 5a and 5b showed the SEM with EDX analysis of both samples after thorough cleaning with concentrated HNO_3. In both cases the metal oxide layer dissolved completely, however the sample exposed to seawater is covered with compact film of oxides, carbonates, sulphides and silicates of divalent metal cations which inhibits general corrosion due to their buffer action prevents the formation of acidity sites[16].

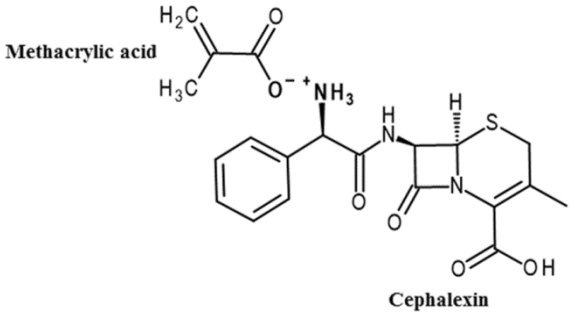

Fig. 4 — SEM and EDX analysis of AA2219-T87 plate immersed for one year duration (a) in 0.6 M NaCl and (b) in seawater before cleaning with HNO_3

Weight loss, pH and electrical conductance measurements

The maximum weight loss in both the cases was observed for 24 h duration (7.1 mpy in 0.6 M NaCl and 6.6 mpy in seawater) and the sample showed improved corrosion resistance when continued up to one year. The higher corrosion rate of AA2219-T87 plate in 0.6 M NaCl solution for 24 h duration is due to the formation of pits in and around the IMPs. It is well known that the Cu particles and Cu-containing intermetallics (Al_2Cu) promote pitting corrosion[17]**.** The higher intensity of Al_2Cu in the alloy surface hampers the formation of a continuous and homogeneous protective oxide layer and thereby resulting more and more severe pitting corrosion[18]. In addition, chloride ions have a strong affinity to secondary phases and its presence increased the solubility of the oxides in turn weakening the passive film. Also, the adsorbed Cl^- ion in the passive oxide film is known to change its electronic and ionic conductivity. These results in passive film heterogeneous distortion in turn reduce the ion resistance of passive film[19]. When the passive film breakdown occurred, large cathode and small anode are formed and thereby accelerating pitting corrosion[20].Furthermore, the metal exposed to 0.6 M NaCl solution after 24 h duration exhibited the *p*H around 7.4, which favoured aluminium oxide/ hydroxide passive film over the aluminium alloy

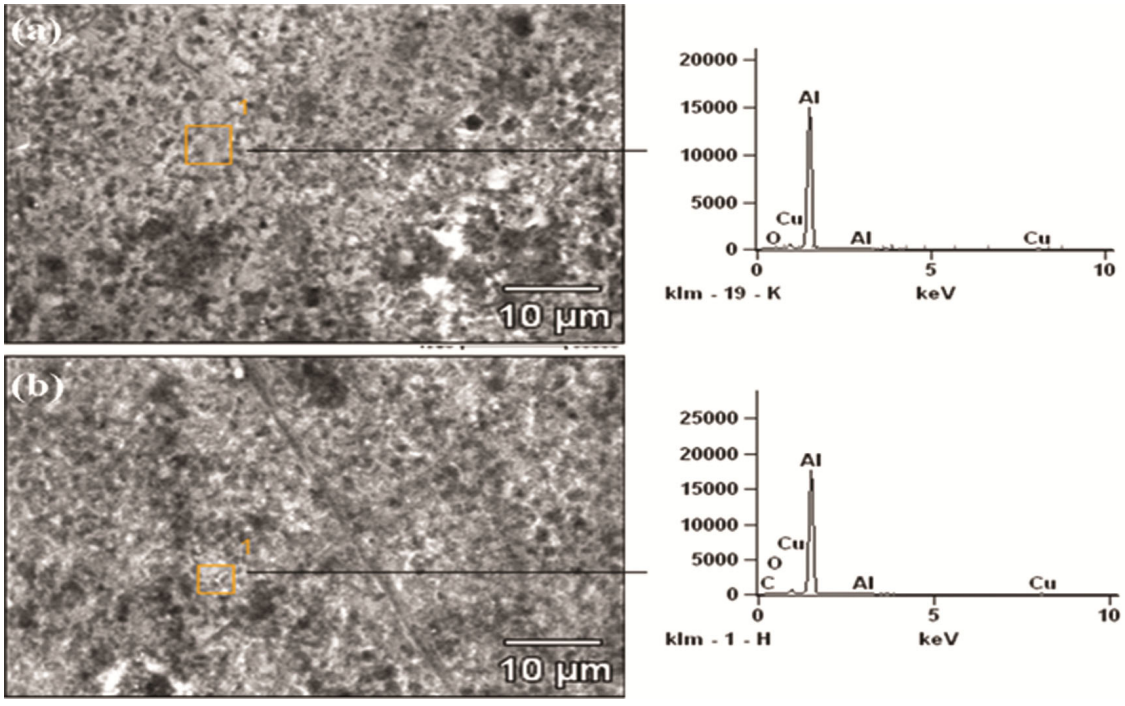

Fig. 5 — SEM and EDX analysis of AA2219-T87 plate immersed for one year duration (a) in 0.6 M NaCl; (b) in seawater after cleaning with HNO_3

surface and improves the corrosion resistance of AA2219-T87 plate (2.3 mpy). However the corrosion rate of AA2219-T87 plate in unsterile seawater showed an improved corrosion resistance than in 0.6 M NaCl solution. This is due to the alkaline nature of seawater (*p*H 8.2) which resulted the formation of passive film over the entire metal surface and showed relatively higher corrosion resistance than 0.6 M NaCl solution (*p*H 6.3). The electrical conductance value of AA2219-T87 plate measured with 0.6 M NaCl solution (38.4 mMho) is due to free movement of ions and responsible for pitting type of corrosion. The slight lower electrical conductance value (33.9 mMho) observed in seawater restricts the movement of aggressive ions in solution in turn prevents direct metal/solution interface. The different parameters obtained from weight loss measurements are given in Table 1.

Electrochemical measurements

The potentiodynamic polarization curves for AA2219-T87 plate in both 0.6 M NaCl and seawater are shown in Fig. 6. The different corrosion parameters obtained from Tafel plots are given in Table 2. The lower corrosion current density (0.15 µA cm^{-2}) obtained from Tafel plots showed the higher corrosion resistance of AA2219-T87 plate in seawater when compared to 0.6 M NaCl solution. In both electrolytes the cathodic slope was higher than anodic slope indicating that the reaction is cathodic control. The cathodic reaction at higher *p*H of seawater causes the dissolution of aluminium via water reduction in turn improves corrosion resistance of 2219-T87 plate according to following reaction (1)[21].

$$Al + 3H_2O + OH^- \rightarrow 3/2\ H_2 + Al(OH)_4^- \quad \ldots (1)$$

This is further confirmed by a slight negative shift in corrosion potential of AA2219-T87 plate in seawater which caused a little passivation over the sample by the formation of aluminium hydroxide. At higher *p*H more passivation was already reported[8].

However in 0.6 M NaCl aerated solution the main cathodic reaction is the oxygen reduction reaction which enhances the corrosion rate of AA2219-T87 plate[15]. Nyquist plot for AA2219-T87 BM in both 0.6 M NaCl and seawater are shown in Fig. 7. The different corrosion parameters obtained from Nyquist plots are given in Table 1. The diameter of semicircle in Nyquist plot corresponding to charge transfer resistance (R_{ct}) and the broad phase angle from Bode phase plot were used as a measure of corrosion rate. The lower charge transfer resistance (28 kΩ cm^2) obtained for the AA2219-T87 sample tested with 0.6 M NaCl confirmed the lower corrosion resistance compared to seawater. This is also in well agreement with previous Tafel plot results and weight loss measurements.

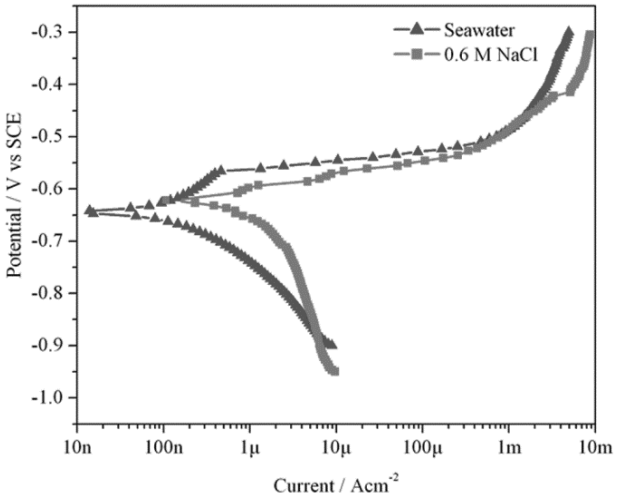

Fig. 6 — Potentiodynamic polarisation curve of AA2219-T87 plate

Table 1 — Weight loss, *p*H and conductance data of AA2219-T87 BM in 0.6 M NaCl and seawater

	Corrosion rate (mpy) in		*p*H in		Conductance (mMho) in	
Duration (days)	NaCl (0.6 M)	Sea water	NaCl (0.6 M)	Sea water	NaCl (0.6 M)	Seawater
0			6.5	8.2	38.4	33.9
1	7.1	6.6	7.3	7.8	39.7	34.9
2	5.7	3.2	7.3	8.0	40.4	35.7
3	5.2	2.4	7.3	7.9	41.8	36.8
4	3.0	0.6	7.2	7.8	43.4	37.8
5	2.5	0.6	7.6	8.1	45.2	39.6
6	2.4	0.6	7.5	8.0	46.5	40.3
7	2.3	0.6	7.5	8.1	49.4	41.6

Table 2 — Corrosion parameters obtained from potentiodynamic polarisation and Nyquist plots

	i_{corr} ($\mu A\ cm^{-2}$)	β_a ($mV\ dec^{-1}$)	β_c ($mV\ dec^{-1}$)	E_{corr} (mV)	R_{ct} ($k\Omega\ cm^2$)	Z ($k\Omega\ cm^2$)
AA2219-T87 plate in seawater	0.15	111	−151	−644	63	48.3
AA2219-T87 plate in 0.6 M NaCl	0.96	33.5	−411	−615	28	23.6

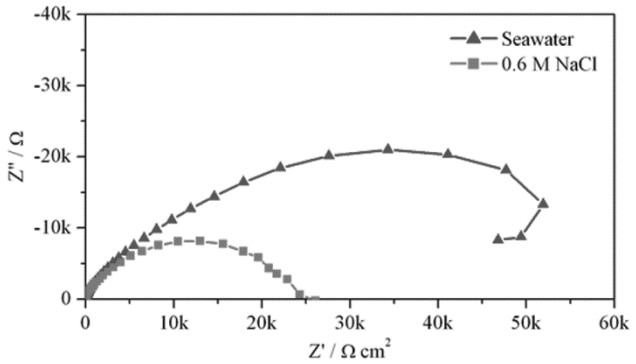

Fig. 7 —Nyquist plot of AA2219-T87 plate

Mechanism of intermetallic dealloying

The AA2219-T87 plate contains Al_2Cuinter-metallicparticles in α-solid solution and the solute elemental copper. The formation of micro galvanic cells with surrounding matrix[22] is responsible for the corrosion of this alloy in both electrolytes. In the corrosion process of metals, the cathodic reaction mechanism is dependent on the *p*H of the media. In presence of oxygen, the reduction reaction (2) occurs in neutral and basic media[23].

$$O_2 + 2H_2O + 4e^- \rightarrow 4OH^- \quad \ldots(2)$$

It has already reported that the oxygen reduction reaction is more favoured on Cu-rich phases[15]. Due to this effect, a high concentration of OH^- ions is generated in turn causes a local increase of *p*H and promotes localized corrosion of the aluminium matrix near the particles[24-27].

$$Al_2Cu \rightarrow Cu + 2Al^{3+} + 6e^- \quad \ldots(3)$$

$$Al_2Cu \rightarrow 2Al^{3+} + Cu^{2+} + 8e^- \quad \ldots(4)$$

Furthermore, a part of dissolved copper may be redeposited to form permanent cathodes which accelerate the dissolution of matrix phase[28].

Conclusion

- The microstructure and corrosion resistance behaviours of AA2219-T87 aluminum alloy plate have been evaluated in aggressive media of unsterile natural seawater and 0.6 M NaCl solution.
- The macrographs and microstructure characterisation reveal complete damage of Al_2Cu intermetallic particlesand redeposition of copper whereas the sample exposed to unsterile seawater show pitting type of corrosion.
- The SEM and EDX images of the sample immersed in seawater for longer duration confirm the presence of magnesium and other minerals in turn caused a slightly higher corrosion resistance of samples.
- The weight loss measurements confirm that the corrosion resistance of AA2219-T87 plate in seawater is higher than in 0.6 M NaCl solution. This is due to the alkaline nature of seawater which favour the formation of passive film over the entire metal surface.
- The electrochemical techniques confirm that the reactions are under cathodic control. The higher cathodic slope favours reduction reaction in the presence of seawater while the lower cathodic slope favours oxygen reduction reaction in 0.6 M NaCl solution.

Acknowledgement

The authors acknowledge Dr. Marie Johnson, President and Dr.Mariazeena Johnson, Chancellor, Sathyabama Institute of Science and Technology, for providing the facilities to carry out the experimental work.

References

1 Schonberg W P, *Acta Astronaut*, 26 (1992) 799.
2 VenkataNarayana G, Sharma V M J, Diwakar V, Sree Kumar K & Prasad R C, *SciTechnol Weld Joi,* 9 (2004) 121.
3 Hosni Ezuber A, El-Houd F, El-Shawesh, *Mater Design,* 29 (2008) 801.
4 Örnek D, Jayaraman A, Wood T K, Sun Z, Hsu C H & Mansfeld F, *Corros Sci,* 43 (2001) 2121.
5 Luklinska Z B & Castle J E, *Corros Sci.* 23 (1983) 1163.
6 Danqing Zhu & Wim J van Ooij, *CorrosSci,* 45 (2003) 2163.
7 Minhua Shao, Yan Fu, Ronggang Hu & Changjian Lin, *Mat Sci Engg A,* 344 (2003) 323.
8 Srinivasa Rao K & Prasad Rao K, *Mat Sci Tech,* 22 (2006) 97.
9 Carla Gouveia-Caridade, Isabel S Pereira M & Christopher M A Brett, *Electrochim Act,* 49 (2004) 785.

10 Shao H B, Wang J M, Wang X Y, Zhang J Q & Cao C N, *ElectrochemComm,* 6 (2004) 6.
11 Kolics A, Besing A S, Baradlai P, Haasch R &Wieckowski A, *J ElectrochemSoc*, 148 (2001) B251.
12 Ferrer K S & Kelly R G, *Corrosion,* 57 (2001) 110.
13 Robinson M J,*CorrosSci,*22 (1982) 775.
14 *Metals Hand Book*, *Properties of Aluminium and Aluminium Alloys*, 10thEdn. 2 (1990) 79.
15 Venkatasubramanian G, Sheik Mideen A, Abhay K Jha&AnbuKulandainathan M, *Mater ChemPhys,*148 *(*2014) 262.
16 Castle J C & Parvizi M S, *Corros Prevent Cont,* 33 (1986) 5.
17 Grilli R, Baker M A, Castle J E, Dunn B & Watts J, *CorrosSci,* 52 (2010) 2855.
18 WeifengXu & Jinhe Liu, *CorrosSci,* 51 (2009) 2743.
19 WeifengXu, Jinhe Liu & Hongqiang Zhu, *ElectrochimActa,* 55(2010) 2918.
20 Gouveia-Caridade C, Isabel M, Pereira S & Brett C M A, *ElectrochimActa,*49 (2004) 785.
21 Dwarakadasa E S, *J ApplElectrochem*, 24 (1994) 911.
22 ValérieGuillaumin& Georges Mankowski, *CorrosSci,* 41 (1999) 421.
23 Aldykiewicz A J, Davenport A J & Isaacs H S, *J Electrochem Soc,* 143 *(*1996) 147.
24 Mazurkiewicz B &Piotrowski A, *CorrosSci,* 23 (1983) 697.
25 Buchheit R G, Grant R P, Hlava P F, McKenzie B & Zender G L, *J ElectrochemSoc,* 144 (1997) 2621.
26 Dimitrov N, Mann J A & Sieradzki K, *J ElectrochemSoc,* 146 (1999) 98.
27 Ilevbare G O & Scully J R, *Corrosion,*57 (2001) 134.
28 Mazurkiewicz B & Piotrowski A, *CorrosSci,* 23 (1983) 697.